Composites Science and Technology 170 (2019) 165–173

Contents lists available at ScienceDirect

Composites Science and Technology

journal homepage: www.elsevier.com/locate/compscitech

Optimization of shear thickening fluid encapsulation technique and dynamic response of encapsulated capsules and polymeric composite

Xin Zhang[a], He Zhang[b], Pengfei Wang[c], Qian Chen[c], Xin Li[d], Youjin Zhou[a], Xinglong Gong[c], Zhong Zhang[e], En-Hua Yang[a,*], Jinglei Yang[f,**]

[a] School of Civil and Environmental Engineering, Nanyang Technological University, 50 Nanyang Avenue, Singapore, 639798, Singapore
[b] The National Engineering Research Center of Novel Equipment for Polymer Processing, The Key Laboratory of Polymer Processing Engineering (SCUT), Ministry of Education, South China University of Technology, Guangzhou, 510641, China
[c] CAS Key Laboratory of Mechanical Behavior and Design of Materials, Department of Modern Mechanics, University of Science and Technology of China, Hefei, 230026, China
[d] National Laboratory of Solid State Microstructures and Department of Materials Science and Engineering, Nanjing University, Nanjing, 210093, China
[e] CAS Key Laboratory of Nanosystem and Hierachical Fabrication, National Center for Nanoscience and Technology, Beijing, 100190, China
[f] Department of Mechanical and Aerospace Engineering, Hong Kong University of Science and Technology, Clear Water Bay, Kowloon, Hong Kong, China

ARTICLE INFO

Keywords:
A. Polymer-matrix composites (PMCs)
B. Impact behavior
C. Deformation
Shear thickening fluid

ABSTRACT

In this work, shear thickening fluid (STF) was fabricated and encapsulated by using three different encapsulation methods for the first time. The mechanical properties of individual STF capsules were investigated to obtain optimal encapsulation method and formula. Much more energy can be absorbed for STF capsules during impact than that of quasi-static compression. The introduction of ultraviolet (UV) curable resin can significantly improve the static strength of STF capsule and thus enhance the handleability of STF capsule. The STF capsules synthesized through the two-step polymerization method show an elastic shell which can stand multiple impacts without any damage. This STF capsule possesses higher static strength and absorbs more strain energy than capsules synthesized through the other two methods. Furthermore, incorporation of the STF capsules into silicone gel enhances the energy absorption capacity of matrix material up to 71.3%.

1. Introduction

Shear thickening fluid (STF) is a non-Newtonian fluid as its shear viscosity increases with the shear load [1,2]. It was first developed by the mixture of cornstarch and water and described in Doctor Seuss's children's book series, as a magic object which could be transferred from liquid state to solid-like state [3]. The phenomenon of shear thickening effect can be explained by Hamaker theory and effect of Van der Waals force. When the shear stress increases, the particles are organized in parallel flows, which reduce the flow's viscosity. When the shear rate rises up to a specific value, however, the hydrodynamic interaction between particles become the dominate factor, which makes the flow of particles difficult resulting in increased viscosity. Due to this unique property, STF has generated a lot of research interests among scientists and researchers [4,5].

The dynamic response of STF in a restrained space has been tested by using a modified Split Hopkinson Pressure Bar (SHPB) [6]. With an obviously increased energy dissipation capacity of STF at high loading rates as compared to the static loading rate, STF has been applied to many fields. For instance, STF has been incorporated in sandwich structures and foam materials to improve their impact resistances [7]. Other researchers used STF as a damping material [8] for vibration control and fatigue endurance. Furthermore, many research has been carried out to investigate the use of STF in body armors due to its promising impact resistance [9]. STF-modified body armors find a balance between the required flexibility of the armor for normal body movements and the protectiveness of the armor upon high speed impacts [10]. For example, many researchers studied the stab resistance of STF treated Nylon and Kevlar fabrics [11–13]. Dramatic improvements in puncture resistance have been observed under high and low speed spike penetration tests. Moreover, significant energy dissipation in the damaged zone has been reported.

Previous studies about the application of STF for body armors were achieved by directly immersing and soaking the fabrics into STF [14].

* Corresponding author.
** Corresponding author.
E-mail addresses: ehyang@ntu.edu.sg (E.-H. Yang), maeyang@ust.hk (J. Yang).

https://doi.org/10.1016/j.compscitech.2018.11.040
Received 6 April 2018; Received in revised form 4 October 2018; Accepted 24 November 2018
Available online 30 November 2018
0266-3538/

However, this approach is not easy to follow because of the high viscosity of STF, which ranges from several Pa·s to several tens Pa·s [15–17]. Some researchers [11] diluted the STF by ethanol for easy application. Excess fluid was removed from the soaked fabric by squeezing and the fabric was dried at an oven to allow evaporation of ethanol. The principal objective of the previous investigations was to explore the feasibility of using STF to enhance the impact resistance of material. Very few studies have been focused on improving the stability of the STF in the fabrics.

In order to overcome the above-mentioned challenges and to increase the stability of STF during its service life, it is of great significance to explore the techniques to tightly package this highly viscous fluid. Among different approaches, encapsulation is the most promising technique because it not only minimizes the mutual influence from the surrounding environment but also makes handling and application of the material much easier [18]. While the techniques are diversified for the encapsulation of solids and liquids with low viscosity [19], it is of great challenge for the encapsulation of STF due to its high viscosity, shear thickening property, and composition of multiple phase ingredients. The only investigation on the encapsulation of liquids with high viscosity (*i.e.*, STF) is our previous work [20], which focuses on the primary attempt of STF encapsulation through a simple fabrication method and performance evaluation of the resulting STF capsule. However, the strength of the capsule shell is low and thus the resulting STF capsule is not easy to handle. Furthermore, performance of STF capsule modified composite (e.g. STF capsule modified polymer) should be investigated to reveal its potential applications.

In this paper, three different encapsulation methods with the aims to enhance the shell strength, to optimize the encapsulation process, and to optimize the energy capacity of STF capsule are explored and compared. Quasi-static compression setup and dynamic impact apparatus were fabricated to characterize the quasi-static and dynamic properties of STF capsules, respectively. High speed camera and field emission scanning electron microscope were employed to characterize the fracture mode and morphology of the STF capsules. STF capsules with the optimized properties were then incorporated into a polymeric matrix for further investigation of the impact performance of the resulting STF capsule modified composites by means of an in-house designed drop weight impact apparatus.

2. Materials and experiments

2.1. Synthesis of PSt-EA particles and preparation of PSt-EA colloidal suspensions

The PSt-EA particles and the PSt-EA colloidal suspensions were synthesized in the lab. The detailed synthesis methods were described in the supporting information. The PSt-EA particles are in spherical shape with a relatively constant diameter of 350 nm (Fig. S1).

2.2. Fabrication of STF capsules

2.2.1. Method 1: single step fabrication

Fabrication of the STF capsules through single step is illustrated schematically in Fig. 1a and was described in detail in our previous work [20]. In the current study, the STF was first diluted with a fixed amount of polyethyleneimine (PEI, 5.0 wt%) and different amount of ethylene glycol (EG), i.e. 5, 10 and 15 wt% (Table S1), for further encapsulation in reaction solutions with chloroform at a pre-determined duration of 5, 30, 60, 120, or 180 min. More fabrication details can be found in the supporting information. For the simple description, STF capsules are denoted as “STF-#-#min” (e.g. STF-85-30min), while the solution is denoted as RS-# (e.g. RS-5.7) according to the amount of chloroform added in the reaction solutions.

2.2.2. Method 2: single step fabrication with NOA 61 infiltration

To increase the shell strength of the STF capsules, the fabricated STF capsules from Method 1 were further treated by infiltrating a layer of ultraviolet (UV) curable resin, NOA 61 (Fig. 1b). Specifically, the pre-fabricated STF capsules were added into 25 or 50 wt% NOA 61 solution in toluene. The capsules fabricated under different condition in Method 2 were denoted as “STF-#-#min-#% NOA” (e.g. STF-85-30min-25% NOA).

2.2.3. Method 3: two-step polymerization

The STF capsules were synthesized using a two-step polymerization method by firstly instilling the diluted STF into immersion solution to stabilize the STF droplets, and then transferring to another reaction solution for the growth of the shell, as can be seen in Fig. 1c. The detailed fabrication method can be found in the supporting information. The function of chloroform in the single step method is multi-functional. It can not only adjust the density of the reaction solution but also can gradually dissolve the redundant EG in the diluted STF. However, the major function of chloroform in the two-step polymerization method is to adjust the density of the immersion solution. Thus, less chloroform is needed in two-step polymerization method, which minimizes the influence of chloroform on STF.

The excess EG in the diluted STF during the encapsulation process is multi-functional. Firstly, since the STF droplet is generated by a syringe, the relative low viscosity of the STF is important for the fabrication process. The viscosity of EG is approximate 0.02 Pa s and remains a constant value [21,22], as shown in Fig. S2. The viscosity of EG is much smaller than the initial viscosity of original STF, which makes it suitable for the dilution of original STF. The excess EG can dramatically decrease the viscosity of the STF, as indicated in Fig. S2. Secondly, the EG will diffuse and dissolve in the external solvent during the reaction which may promote the formation of the inner shell of the STF capsule, which can significantly increase the robustness of the capsule. It can also help to remove the excess EG to achieve the shear thickening effect, which is most important in the STF encapsulation technique. Last but not least, the EG can react with Suprasec 2644 to thicken the outer shell to further improve the robustness of the capsule.

Fig. 1d and e compares the STF capsules fabricated through Method 1 and Method 2. All capsules are in spherical shape with smooth surface and relatively constant diameters. The average diameter for STF capsules from both Methods 1 and 2 is 2.63 mm, while that from Method 3 is 2.56 mm. STF is successfully encapsulated in the polymer shell as large amount of STF liquid comes out when capsules are fractured as shown in the green square frame.

2.3. Fabrication of STF capsule modified polymer

To demonstrate potential application of the newly fabricated STF capsules, performance of STF capsule modified silicone gel was evaluated. 13.9% of STF capsules by volume were uniformly dispersed into the fresh gel by hand mixing. The mixture was then poured into cylindrical molds. The fabricated samples are cylindrical in shape with diameter around 13 mm and height around 6 mm.

2.4. Experiments

2.4.1. Rheological measurements

The viscosity of fabricated STF was measured by a rheometer as described in the supporting information. As can be seen in Fig. S2, the initial viscosity of the suspension is about 8 Pa s and the viscosity of the STF decreases slightly with shear rate at low shear rate range. A dramatically increase of viscosity can be observed when the shear rate is beyond 550 s^{-1}. The viscosity can reach 115 Pa s at a shear rate of 680 s^{-1}, which indicates that the PSt-EA suspension possesses strong shear thickening properties.

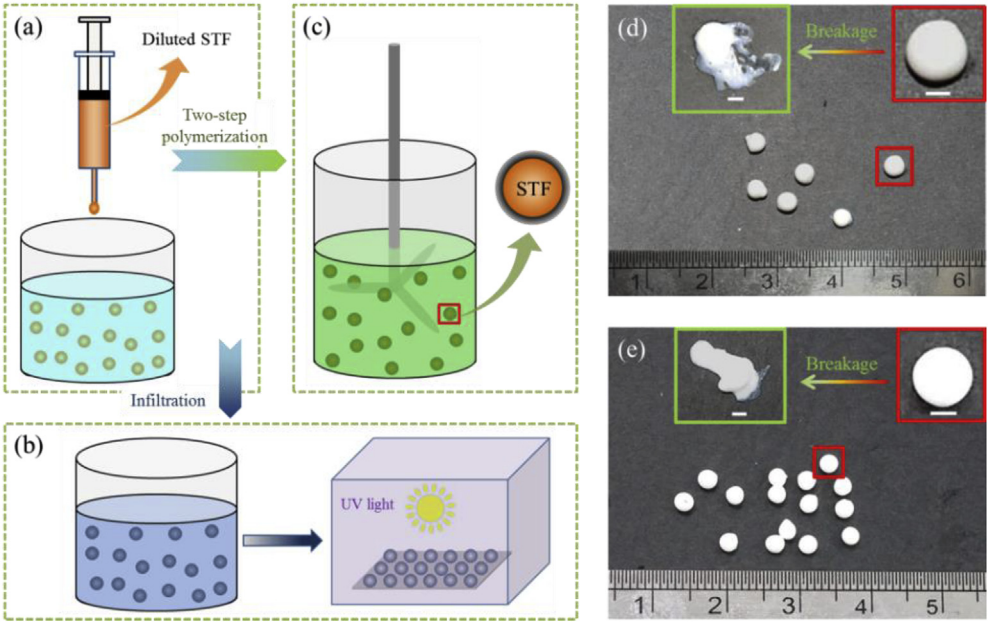

Fig. 1. Schematic illustration of STF capsules fabrication: (a) Method 1, (b) Method 2, and (c) Method 3; STF capsule from (d) Method 1 (STF-85-30min) and (e) Method 3 (scale bar in white represents 1 mm).

2.4.2. Quasi-static compression test

A punch head connected to a load cell was used to carry out the quasi-static compression of the STF capsules, as schematically depicted in Fig. 2a. The loading speed was controlled at 10 μm/s by an actuator. The corresponding strain rate (0.005 s^{-1}) is calculated by dividing the loading speed by the capsule diameter. The nominal stress is defined as the load divided by the cross sectional area at the equatorial position of the capsule, while the nominal strain is defined as the deformation divided by the diameter of the capsule. The nominal strength is defined as the peak stress divided by the equator cross sectional area of the capsule [23].

2.4.3. Dynamic compression test

In order to evaluate the dynamic properties of the STF capsules, a dynamic compression apparatus is developed, as schematically shown in Fig. 2b. The detailed description of the apparatus can be found in the supporting information. Four impact velocities, 1.5, 2.1, 2.55, and 2.95 m/s, are used to evaluate the loading rate effects. Deformation of the capsule can be obtained by integrating the velocity-time curve of impactor (see supporting information).

2.4.4. Drop weight impact test

A T-shape impactor with a mass of 149 g was manufactured to evaluate the mechanical properties of STF capsule modified silicone gel, as schematically shown in Fig. 2c. The aluminum plate with a diameter of 50 mm was fixed on an aluminum bar with a diameter of 12.7 mm. The impactor drops freely through a slide guide to generate impact at a velocity of approximate 1.4 m/s. Two PVDF films were used to determine the load and time during the impact. The lower PVDF film was calibrated with a SHPB [24]. It was placed between the incident and

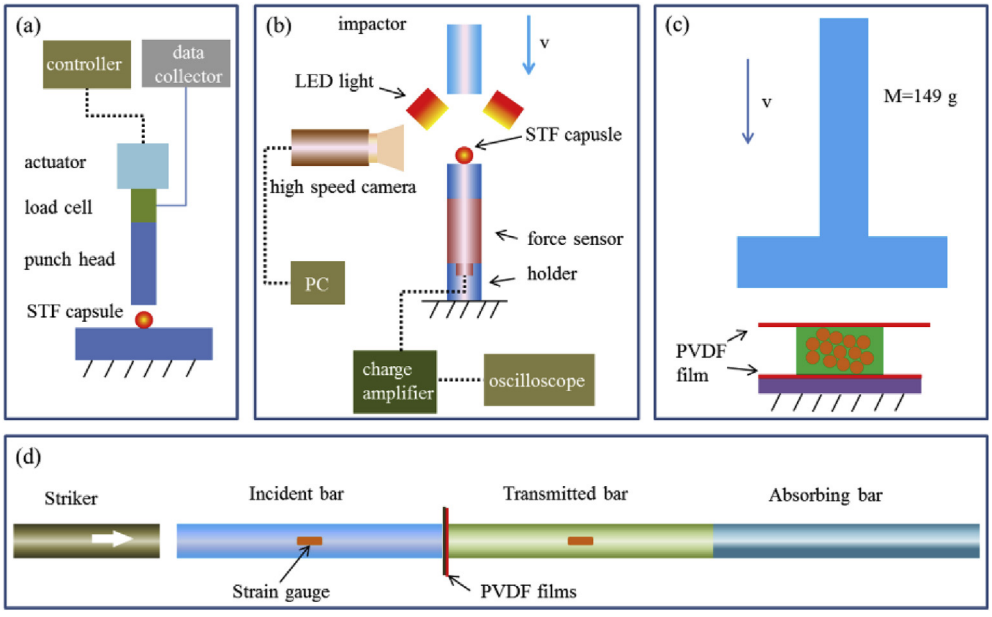

Fig. 2. (a) Quasi-static compression apparatus, (b) dynamic compression apparatus, (c) drop weight impact tester, and (d) SHPB for the calibration of PVDF films.

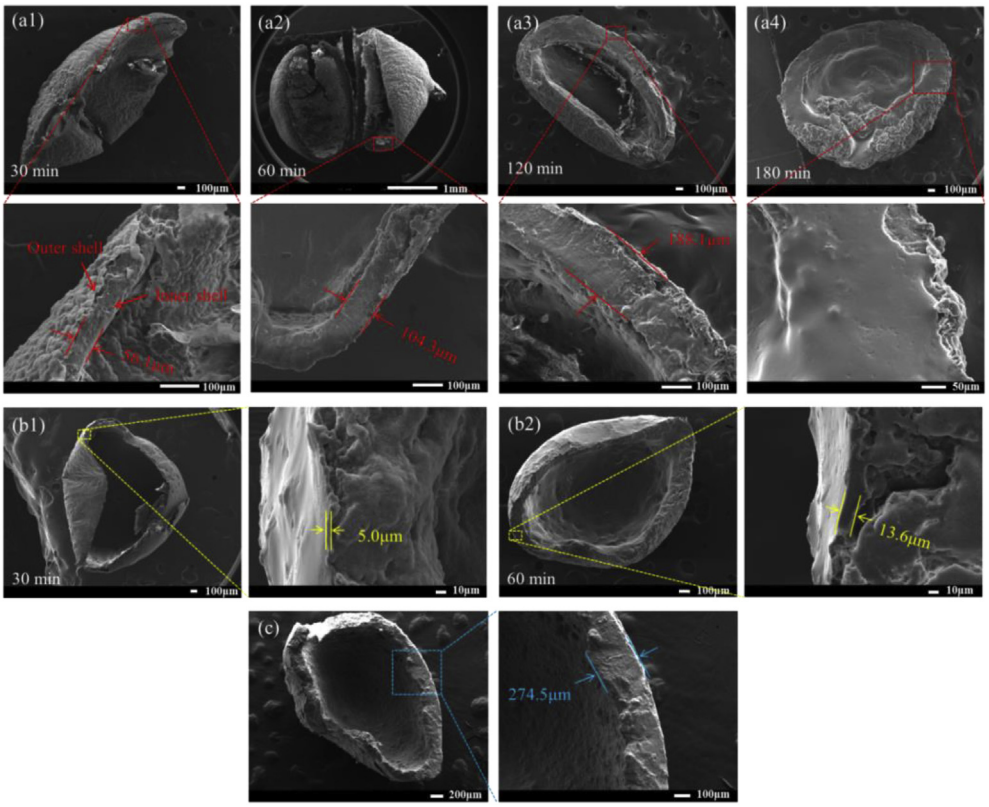

Fig. 3. SEM images of (a1) STF-85-30min, (a2) STF-85-60min, (a3) STF-85-120min, and (a4) STF-85-180min capsule (Method 1); profiles of (b1) STF-85-30min-50% NOA and (b2) STF-85-60min-50% NOA capsules (Method 2); (c) profiles of STF-70 capsules (Method 3).

transmitted bars for the calibration, as can be seen in Fig. 2d. The amplification factor K of the PVDF film is calculated to be 126 by comparing the signals obtained from PVDF film with loads measured from SHPB (Fig. S4) at different impact velocities.

3. Results and discussion

3.1. Morphology of STF capsules

Fig. 3 shows the morphology of STF capsules fabricated through three different methods. A double-walled structure for STF-85 capsule from Method 1 is formed during the fabrication process, which consists of inner shell and outer shell (Fig. 3a). The outer shell is polyurea while the inner shell is condensed PSt-EA particles due to the reaction between EG in the STF and Suprasec 2644. As a result, EG is consumed and PSt-EA particles are accumulated at the interface to form inner shell. The outer shell is a dense membrane which is much thinner than the inner shell. The shell thickness increases significantly with increasing reaction time due to the continuous polymerization at interface which leads to further accumulation of the PSt-EA nano-particles. Prolonged reaction duration of 180 min (Fig. 3a4) with very thick shell thus is not suitable for STF encapsulation.

Fig. 3b shows the STF capsules from the method 2. The outer shell is coated with NOA. The shell of STF-85-60min-50% NOA is thicker than that of STF-85-30min-50% NOA due to longer reaction duration. The outer shell of STF-85-60min-50% NOA capsule (13.6 μm) is almost three times that of STF-85-30min-50% NOA (5 μm). Since NOA 61 is relatively strong, the compact composite outer shell should increase the strength of capsule and makes handling easier for applications. Furthermore, Fig. 3c shows the profile of STF-70 capsules from the two-step polymerization method. It also consists of inner shell and outer shell and the overall thickness is about 274.5 μm which may provide robust mechanical property of the capsule. Although the shell thickness of the capsule from Method 3 is a little bit larger than that from Method 1 (e.g., STF-85%-120min), it can still encapsulate sufficient STF than the STF-85%-180 min which is beneficial for the energy absorption.

3.2. Influence of key parameters for the single step encapsulation process (Method 1)

The reaction duration and chloroform concentration are key parameters for the single step encapsulation (Method 1). Different amount of STF (*i.e.,* STF-80, STF-85, and STF-90) was used in the same reaction solution (*i.e.,* RS-5.7). The STF-90 droplets in RS-5.7; however, solidified rapidly in less than 30 min due to the low dosage of EG (*i.e.,* 5 wt%) in the STF-90. Consequently, the STF-90 capsules were fabricated in RS-4.7 for comparison. Fig. 4a shows the nominal strength under quasi-static compression for capsules with respect to different reaction duration. The quasi-static nominal strengths of all capsules increase with reaction duration. This is attributed to increased shell thickness with prolonged reaction duration as shown in Fig. 3a. Moreover, increased concentration of STF results in higher quasi-static nominal strength as STF-90 capsule exhibits significantly higher strength.

Fig. 4b shows the typical nominal stress versus nominal strain curves under dynamic loading (2.95 m/s) for STF-80. The peak stress decreases with reaction duration due to more energy can be absorbed by the capsule with prolonged reaction duration which leads to less residual impact energy of the impactor to cause smaller peak load. The nominal stress of capsules in the plateau stage increases gradually with the increased reaction duration. The densification strain (ε_D) can be determined by the intersection of tangents to the stress-strain curve for the impact region and densification region, as indicated in red dash lines in Fig. 4b [25]. The nominal strain energy under dynamic impact is obtained by calculating the area under the stress-strain curve up to strain of 0.5 through integration to ensure the strain energy is absorbed before the densification of the capsule.

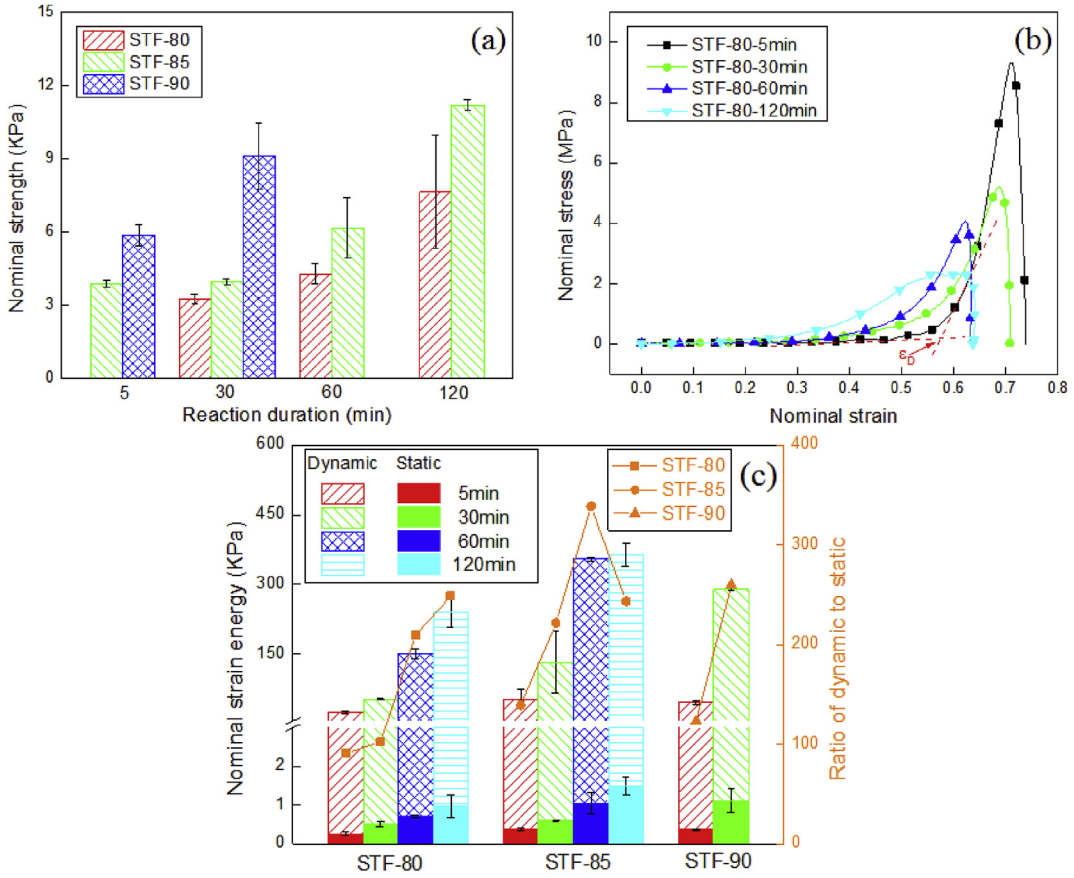

Fig. 4. (a) Nominal strength under quasi-static compression, (b) typical nominal stress versus nominal strain curve of STF-80 capsules under dynamic loading, and (c) static and dynamic nominal strain energy and dynamic-to-static strain energy ratio of STF capsules as a function of STF dosage and reaction durations.

Fig. 4c shows the absorbed nominal strain energy under quasi-static loading and dynamic impact (2.95 m/s) for STF-80, STF-85, and STF-90 capsules with respect to different reaction duration. The nominal strain energy absorptions under quasi-static loading are calculated by integrating the entire area under the stress-strain curve till the catastrophic failure of the tested capsule. As can be seen, the static nominal strain energy increases moderately with reaction duration due to prolonged reaction duration increases shell thickness and improves robustness of both inner and outer shells. It was observed that much more strain energy can be absorbed under impact than static loading for all capsules. The dynamic nominal strain energy increases with both increasing STF dosage and reaction. This is attributed to more EG is consumed with the reaction duration to perform good shear thickening effect and higher dosage of STF may also help improve shear thickening effect.

Fig. 4c also compares the shear thickening capacities of the resulting STF capsules by plotting the ratio of the dynamic strain energy to the static strain energy. As can be seen, the dynamic-to-static strain energy ratio generally increases with reaction duration and STF dosage. For STF-85, the dynamic-to-static strain energy ratio peaks at 60 min reaction duration and decreases for prolonged reaction duration. This is because with the increase of reaction duration, the static strength of the resulting capsule may increase and the STF in the core may reduce which leads to the decrease of the dynamic-to-static ratio. Overall, the STF-85-60min capsule possesses the highest dynamic-to-static strain energy ratio of 338 and high dynamic nominal strain energy absorption capacity of 350 KPa, and thus is considered the optimized synthesis condition of Method 1. The STF-85-60min capsule was selected for further investigation and comparison with capsules synthesized from the other two methods.

No evident shear thickening effect of diluted STF (STF-85-dilluted) can be found in the enlarged figure in Fig. S2. The viscosity decreases at the initial stage and remains at around 0.3 Pa s which is a quite low value. In this situation, the STF capsule with very short time reaction duration can be regarded as specimen with little or no shear thickening effect. As shown in Fig. 4c, lower ratio of dynamic to static can be found in STF-85-5min capsules while much higher ratio can be found in STF-85-60min capsule. This phenomenon can prove that the shear thickening effect of the core material dominates the energy absorption capacity of the STF capsules.

In order to further understand the state of the fluid inside the capsules. The fabricated STF-85-60min capsules with good energy absorption capacity were squeezed and the core liquid was collected to carry out the rheological test. Fig. S2 shows an evident shear thickening effect for the squeezed core material of STF-85-60min capsules which can directly prove that shear thickening effect can be achieved after the encapsulation process. However, it is worth noting that, the shear thickening effect of the STF after 60min reaction is not as strong as the original STF and the critical shear rate of the STF after reaction is larger than the original STF. There are many reasons to explain such phenomenon. It is known that the volume fraction of the particles in the STF influences the shear thickening effect and the critical shear rate [26]. The volume fraction of the particles in the STF after reaction may vary from that of the original STF. Another reason can be explained as the collected core liquid may absorb moisture during the squeezing of the capsules, which may influence the shear thickening effect. The agglomeration of the particles to the inner shell may affect the distribution of the particles in the STF mixture, which may also decrease the shear thickening effect.

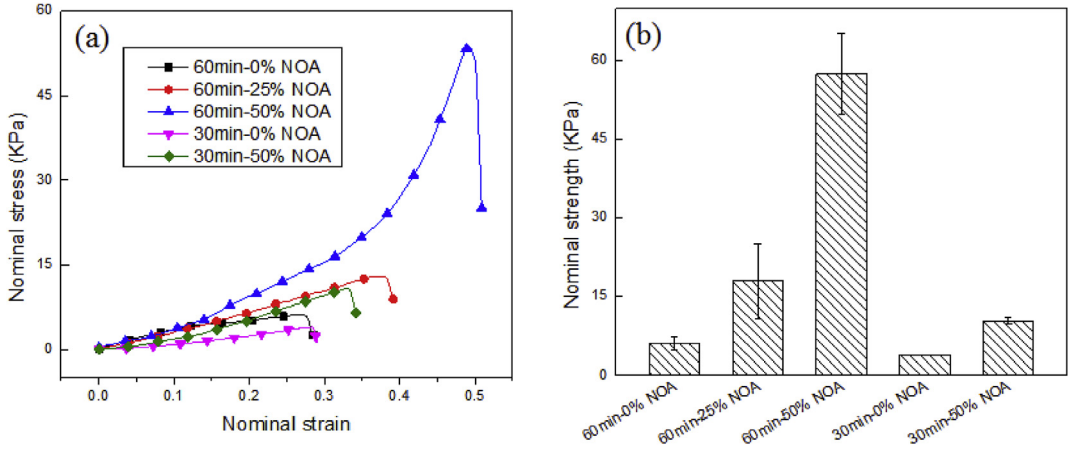

Fig. 5. (a) Typical nominal stress-strain curves and (b) nominal strength of NOA infiltrated STF-85 capsules subjected to quasi-static compression.

3.3. Influence of reaction duration and infiltration factor in Method 2

To improve the handleability of capsules, the STF-85 capsules were further treated with NOA 61 (UV curable resin) in Method 2. Fig. 5a plots the typical nominal stress-strain curves of NOA treated STF-85 capsules subjected to quasi-static loading. The nominal stress increases with nominal strain and a sudden load drop at the peak stress indicates catastrophic failure of capsule. The quasi-static strength of STF-85 capsule increases with increasing NOA 61 dosage, which suggests the introduction of NOA 61 infiltration improves the strength of capsule and thus enhances the handleability of capsule. Enhancement of the quasi-static nominal strength; however, is much more pronounced for the STF-85-60min capsules (9.3 times enhancement) than that for the STF-85-30min capsules (2.6 times enhancement). Since the outer shell of STF-85 capsule is quite thin (~ 1 μm), the NOA 61 can be absorbed in the shell. As a result, the thick shell of the STF-85-60min capsule (Fig. 3b) may absorb more NOA 61 during the infiltration.

Typical dynamic stress-strain curves of NOA infiltrated STF-85 capsules are shown in Fig. 6a and b. The stiffness at lower strain level (*i.e.,* 0.2–0.4 strain) increases significantly with prolonged reaction duration (Fig. 6a) due to the increase of the shell strength. The energy absorption capacity (up to 0.5 strain) increases from 0.095 MPa to 0.396 MPa (Fig. 6c), which reveals that the prolonged reaction duration is necessary to fabricate the STF with strong shear thickening effect that can absorb more energy during impact. However, the peak stress reduces with increasing reaction duration because more impact energy is consumed by the capsule with prolonged reaction duration which leads to less residual impact energy of the impactor to generate smaller peak load in the densification. Effects of NOA dosage on the dynamic responses of NOA infiltrated STF-85 capsules are presented in Fig. 6b. The STF-85-60min-25% NOA capsules have similar dynamic stress-strain behavior with the STF-85-60min-0% NOA capsules, while the STF-85-60min-50% NOA capsules show slightly reduced peak stress and moderately enhanced energy absorption capacity (Fig. 6c). This is attributed to the strength increase may help the capsule to absorb more impact energy which leads to peak stress decrease. In summary, the infiltration of hardened UV curable resin on the surface of the STF capsules (Method 2) leads to significant increase of the static strength (Fig. 5b) and hence the handleability of STF capsules; however, it does not cause remarkable improvement of the dynamic strain energy absorption capacity (Fig. 6c), which implies that most of the impact energy was absorbed by the core material rather than the shell material. Based on the results of STF-85 capsules, 50% NOA dosage is necessary in Method 2 for meaningful modification of shell properties of the STF-85 capsules.

3.4. Performance of STF capsules synthesized through two-step polymerization (Method 3)

Fig. 7a illustrates typical nominal stress-strain curves of STF capsules synthesized through Method 3. Under quasi-static loading, catastrophic failure is observed after a steady increase of nominal stress. The static strength of the STF capsule synthesized in the Method 3 (160 KPa) is about three times that of the best capsule (STF-85-60min-50% NOA) fabricated through Method 2. Under impact loading, the peak stress increases with increasing impact velocity and it was observed that the capsules did not break after impact. Fig. 7b demonstrates the dynamic nominal stress-strain curves of the STF-70 capsules

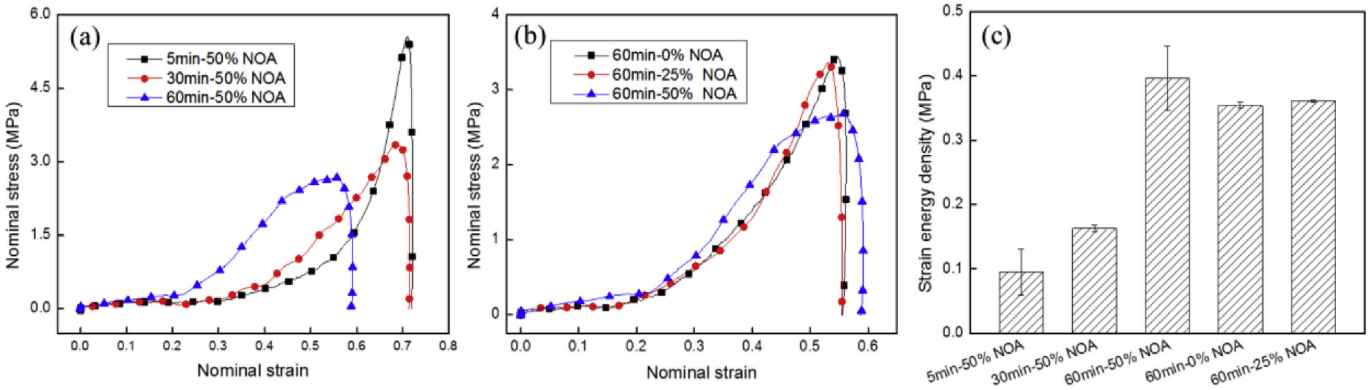

Fig. 6. Typical nominal stress-strain curves of NOA infiltrated STF-85 capsules as a function of (a) reaction duration and (b) NOA dosage subjected to impact loading; and (c) dynamic strain energy density of NOA infiltrated STF-85 capsules.

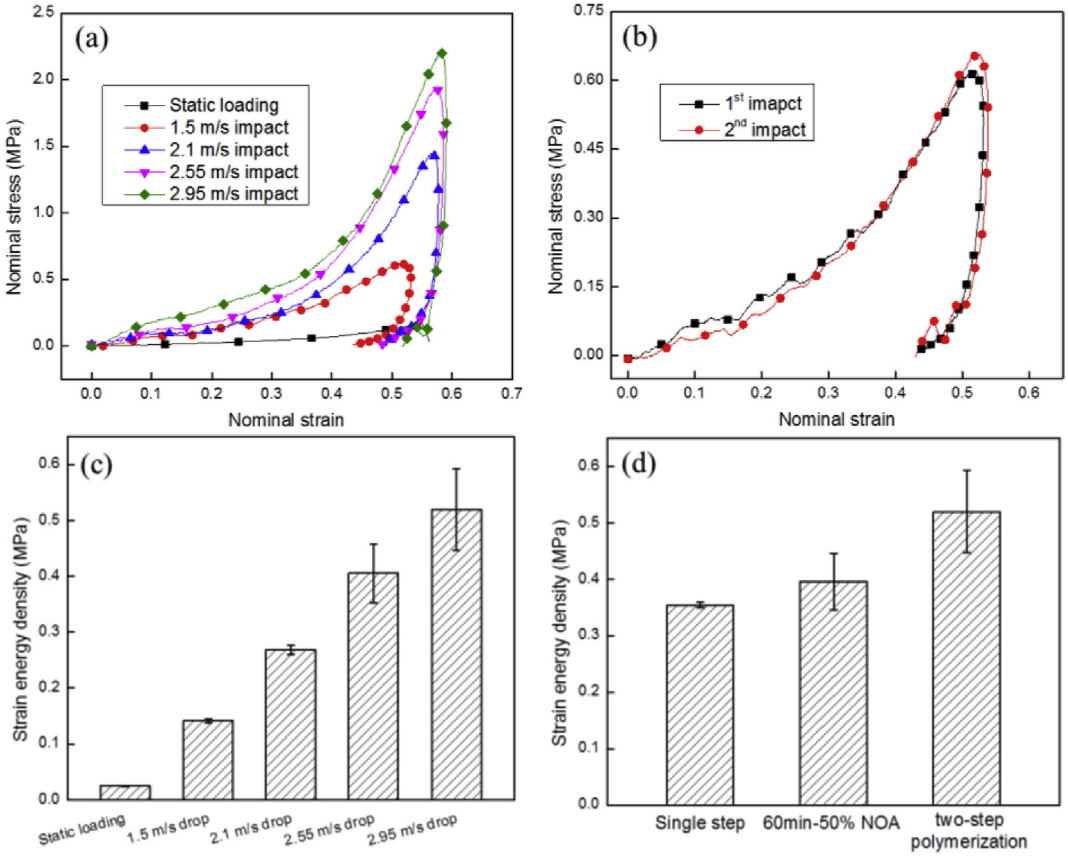

Fig. 7. (a) Typical static and dynamic nominal stress-strain curves of the STF capsules (method 3), (b) dynamic nominal stress-strain curves of the STF capsules (method 3) subjected to repeated impacts, (c) strain energy density of STF capsules (method 3) as a function of loading rate, and (d) strain energy density of STF capsules synthesized from different methods.

subjected to repeated impacts (1.5 m/s). The nominal stress-strain curve subjected to the 2nd impact is similar to that subjected to the 1st impact. This suggests the STF capsules synthesized through Methods 3 can withstand impact loading and recover completely without any damage. All the impact energy can be absorbed by the capsule synthesized through Method 3 as no fracture occurs in the capsule during the impact. As a result, the strain energy absorption is defined as the area of the integral nominal stress-strain curve, which is a little different with the definition of strain energy absorption of capsules from Method 1 and 2 as defined in Session 3.2. The strain energy absorption of STF capsule synthesized through Methods 3 increases dramatically with increasing loading velocity (Fig. 7c). Fig. 7d compares the strain energy absorption capacity of STF capsules synthesized from three methods subjected to the same impact loading (2.95 m/s). As can be seen, STF capsules synthesized through two-step polymerization method show much more energy absorption than the other two methods.

3.5. Deformation and fracture modes of STF capsules

Fig. 8 compares the deformation morphology of capsules with NOA infiltration and capsules synthesized from Method 3 [noted that the deformation morphology of capsules without NOA infiltration (i.e., from Method 1) is similar to that of capsules with NOA infiltration]. The time interval between each row in the blue square frame is 400 μs. For Fig. 8a series, an apparent unstable state can be observed in Fig. 8a2 as the top and bottom surfaces of the capsule are not symmetrical. The core liquid leaks out after the breakage of the shell (Fig. 8a4), which indicates that the diluted STF with only 5min reaction stills behave like liquid during the impact loading. This also provides evidence that no obvious shear thickening effect can be obtained from STF-5min-50% NOA capsule. However, equilibrium state can be found during the entire impact process of STF-85-60min-50% NOA capsule. The capsule fractures after the initial contact with the impactor, as indicated by the red arrow in Fig. 8b2. Through the fracture shell, it can be found that the core material in STF-60min-50% NOA capsule keeps solid state during the impact, which indicates that the core material can provide sufficient shear thickening effect during impact loading. It can also explain why higher stress can be observed during the impact of the STF-60min-50% NOA capsule than other capsules, as shown in Fig. 6a. After 1.186 s, the STF return to the liquid state to wet the surface of damaged specimen due to the capillary effect. A similar equilibrium state has also been found in capsule fabricated through Method 3 (Fig. 8c series). No fracture or damage is observed during the impact and the impactor rebounds after the impact (Fig. 8c4). The STF capsule recovers its shape slowly after removing the impact load.

3.6. Impact resistance of STF capsule modified silicone gel

The STF capsules synthesized through Method 3 possesses the highest static strength and absorbs the most strain energy among all capsules, and thus were used to fabricate STF capsules modified silicone gel. Fig. 9a compares the integral typical stress-strain curves of pure silicone gel specimen and STF capsule modified silicone gel composite subjected to drop weight impact. The integral stress-strain curve can be divided into two distinctive stages. The first stage is only generated because of the compression of the specimen. The second stage is generated because of the densification of the material and the structural property. The mechanical performance of specimen at the second stage is not considered in this study. The two stages can be identified by the

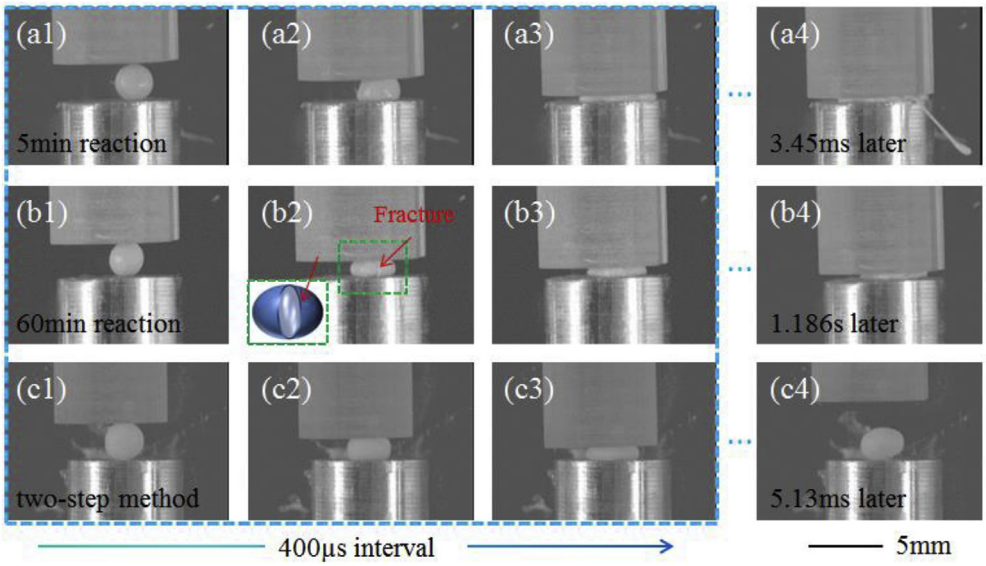

Fig. 8. Deformation of (a) STF-85-5min-50% NOA capsule, (b) STF-85-60min-50% NOA capsule, and (c) STF capsule (method 3) with the time interval of 400 μs.

densification strain (ε_D) of the material, which is determined by using the intersection of tangents to the stress-strain curve. As seen from Fig. 9b that the silicone gel exhibits lower first stage stress while the STF capsule modified silicone gel behaves significantly higher first stage stress, which indicates that the embedded STF capsules may exert their shear thickening properties and improve the impact resistance of composite. Higher peak stress has been observed for pure silicone gel at the second stage. The velocity of the impactor will decrease to zero after each impact due to the impact resistance of the material. The silicone gel specimen may not provide sufficient impact resistance during the impact which may generate larger peak stress and larger strain during the densification stage of the material. The strain energy per unit density is used to investigate the energy absorption capacity of the STF capsule filled silicone gel. The strain energy per unit density is evaluated by the integration of the stress-strain curve up to strain of 0.6 to guarantee that all the impact energy absorbed is within the first stage of

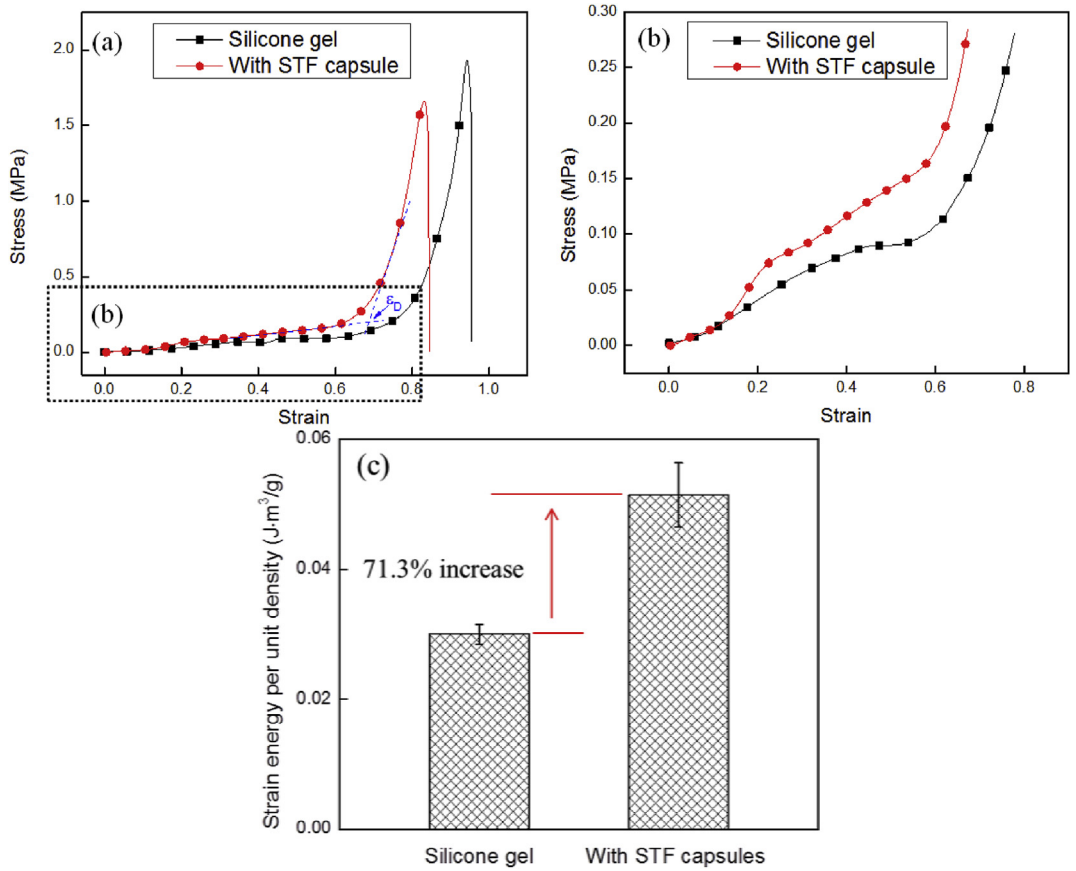

Fig. 9. (a) Stress-strain curves, (b) enlarged stress-strain curves in the black frame, and (c) strain energy per unit density of neat silicone gel and STF capsule modified silicone gel subjected to impact loading.

the material, and then divides the density of the sample. As can be seen in Fig. 9c, the strain energy per unit density for silicone gel is only 0.030 $J{\cdot}m^3/g$ while that of the STF capsule modified silicone gel composite is 0.051 $J{\cdot}m^3/g$, a 71.3% enhancement of energy absorption capacity. This suggests that the introduction of STF capsules into polymer matrix can be regarded as a significant modification for the purpose of impact resistance applications.

4. Conclusions

STF that consists of PSt-EA particles and EG was fabricated in the lab to achieve an outstanding shear thickening effect. The STF was encapsulated by using three different methods for easy handling. Quasi-static compression and dynamic impact apparatuses were established. The UV curable resin increases the quasi-static strength and energy absorption capacity of STF capsules. The STF capsules synthesized through Method 3 shows an elastic shell which can stand the multiple impacts without any damage. Furthermore, this STF capsule possesses higher static strength and absorbs more strain energy than capsules synthesized through the other two methods. Different deformation and fracture modes have been identified for STF capsules fabricated through different methods. Different from STF capsules infiltrated with UV curable resin, no damages can be found in STF capsules from Method 3 even under higher velocity impact. Moreover, the STF capsules can also enhance the impact resistance of silicone gel significantly. The energy absorption capacity has increased 71.3% after the incorporation of STF capsules.

Acknowledgements

Jinglei Yang acknowledges the financial support of the HKUST Start-up fund (R9365). Xin Zhang is grateful for the IGS scholarship from NTU.

Appendix A. Supplementary data

Supplementary data to this article can be found online at https://doi.org/10.1016/j.compscitech.2018.11.040.

References

[1] E. Brown, N.A. Forman, C.S. Orellana, H.J. Zhang, B.W. Maynor, D.E. Betts, J.M. DeSimone, H.M. Jaeger, Generality of shear thickening in dense suspensions, Nat. Mater. 9 (3) (2010) 220–224.
[2] H.A. Barnes, Shear-thickening (dilatancy) in suspensions of nonaggregating solid particles dispersed in Newtonian liquids, J. Rheol. 33 (2) (1989) 329–366.
[3] N.J. Wagner, J.F. Brady, Shear thickening in colloidal dispersions, Phys. Today 62 (10) (2009) 27–32.
[4] C. Fischer, S.A. Braun, P.E. Bourban, V. Michaud, C.J.G. Plummer, J.A.E. Manson, Dynamic properties of sandwich structures with integrated shear-thickening fluids, Smart Mater. Struct. 15 (5) (2006) 1467–1475.
[5] C.D. Cwalina, C.M. McCutcheon, R.D. Dombrowski, N.J. Wagner, Engineering enhanced cut and puncture resistance into the thermal micrometeoroid garment (TMG) using shear thickening fluid (STF) - armor (TM) absorber layers, Compos. Sci. Technol. 131 (2016) 61–66.
[6] W.F. Jiang, X.L. Gong, S.H. Xuan, W.Q. Jiang, F. Ye, X.F. Li, T.X. Liu, Stress pulse attenuation in shear thickening fluid, Appl. Phys. Lett. 102 (10) (2013).
[7] M. Soutrenon, V. Michaud, Impact properties of shear thickening fluid impregnated foams, Smart Mater. Struct. 23 (3) (2014) 035022.
[8] R.C. Neagu, P.-E. Bourban, J.-A.E. Månson, Micromechanics and damping properties of composites integrating shear thickening fluids, Compos. Sci. Technol. 69 (3) (2009) 515–522.
[9] W. Li, D.S. Xiong, X.D. Zhao, L.L. Sun, J. Liu, Dynamic stab resistance of ultra-high molecular weight polyethylene fabric impregnated with shear thickening fluid, Mater. Des. 102 (2016) 162–167.
[10] Z.Q. Lu, X.Y. Jing, B.Z. Sun, B.H. Gu, Compressive behaviors of warp-knitted spacer fabrics impregnated with shear thickening fluid, Compos. Sci. Technol. 88 (2013) 184–189.
[11] M.J. Decker, C.J. Halbach, C.H. Nam, N.J. Wagner, E.D. Wetzel, Stab resistance of shear thickening fluid (STF)-treated fabrics, Compos. Sci. Technol. 67 (3–4) (2007) 565–578.
[12] Y. Park, Y. Kim, A.H. Baluch, C.G. Kim, Empirical study of the high velocity impact energy absorption characteristics of shear thickening fluid (STF) impregnated Kevlar fabric, Int. J. Impact Eng. 72 (2014) 67–74.
[13] I. Kartsonakis, I. Daniilidis, G. Kordas, Encapsulation of the corrosion inhibitor 8-hydroxyquinoline into ceria nanocontainers, J. Sol. Gel Sci. Technol. 48 (1–2) (2008) 24–31.
[14] M. Hasanzadeh, V. Mottaghitalab, H. Babaei, M. Rezaei, The influence of carbon nanotubes on quasi-static puncture resistance and yarn pull-out behavior of shear-thickening fluids (STFs) impregnated woven fabrics, Compos. Appl. Sci. Manuf. 88 (2016) 263–271.
[15] A. Laha, A. Majumdar, Interactive effects of p-aramid fabric structure and shear thickening fluid on impact resistance performance of soft armor materials, Mater. Des. 89 (2016) 286–293.
[16] H. Barnes, Shear-thickening ("Dilatancy") in suspensions of nonaggregating solid particles dispersed in Newtonian liquids, J. Rheol. 33 (2) (1989) 329–366 (1978-present).
[17] S.R. Raghavan, S.A. Khan, Shear-thickening response of fumed silica suspensions under steady and oscillatory shear, J. Colloid Interface Sci. 185 (1) (1997) 57–67.
[18] H.F. Chan, S. Ma, J. Tian, K.W. Leong, High-throughput screening of microchip-synthesized genes in programmable double-emulsion droplets, Nanoscale 9 (10) (2017) 3485–3495.
[19] S.S. Lee, B. Kim, S.K. Kim, J.C. Won, Y.H. Kim, S.H. Kim, Robust microfluidic encapsulation of cholesteric liquid crystals toward photonic ink capsules, Adv. Mater. 27 (4) (2015) 627–633.
[20] H. Zhang, X. Zhang, Q. Chen, X. Li, P. Wang, E.-H. Yang, F. Duan, X. Gong, Z. Zhang, J. Yang, Encapsulation of shear thickening fluid as an easy-to-apply impact-resistant material, J. Mater. Chem. A 5 (43) (2017) 22472–22479.
[21] K.K. Fu, H.J. Wang, L. Chang, M. Foley, K. Friedrich, L. Ye, Low-velocity impact behaviour of a shear thickening fluid (STF) and STF-filled sandwich composite panels, Compos. Sci. Technol. 165 (2018) 74–83.
[22] G. Elert, Viscosity–The Physics Hypertextbook, The Physics Hypertextbook, [Online]. Available: http://physics.info/viscosity/.[Accessed 04 05 2015].
[23] X. Zhang, P.F. Wang, D.W. Sun, X. Li, T.X. Yu, E.H. Yang, J.L. Yang, Rate dependent behaviors of nickel-based microcapsules, Appl. Phys. Lett. 112 (22) (2018).
[24] J. Xu, P. Wang, H. Pang, Y. Wang, J. Wu, S. Xuan, X. Gong, The dynamic mechanical properties of magnetorheological plastomers under high strain rate, Compos. Sci. Technol. 159 (2018) 50–58.
[25] A. Paul, U. Ramamurty, Strain rate sensitivity of a closed-cell aluminum foam, Mater. Sci. Eng. Struct. Mate. Prop. Microstruct. Process. 281 (1–2) (2000) 1–7.
[26] Y.S. Lee, E.D. Wetzel, N.J. Wagner, The ballistic impact characteristics of Kevlar (R) woven fabrics impregnated with a colloidal shear thickening fluid, J. Mater. Sci. 38 (13) (2003) 2825–2833.